Isomerization of *all-trans*-Retinol to *cis*-Retinols in Bovine Retinal Pigment Epithelial Cells: Dependence on the Specificity of Retinoid-Binding Proteins†

Joshua K. McBee,‡,|| Vladimir Kuksa,‡ Rosana Alvarez,§ Angel R. de Lera,§ Oleg Prezhdo,|| Françoise Haeseleer,‡ Izabela Sokal,‡ and Krzysztof Palczewski*,‡,||,⊥

Departments of Ophthalmology, Chemistry, and Pharmacology, University of Washington, Seattle, Washington 98195, and Departmento de Quimica Organica, Universidade de Vigo, 36200 Vigo, Spain

Received May 9, 2000; Revised Manuscript Received July 5, 2000

ABSTRACT: In the retinal rod and cone photoreceptors, light photoactivates rhodopsin or cone visual pigments by converting 11-*cis*-retinal to *all-trans*-retinal, the process that ultimately results in phototransduction and visual sensation. The production of 11-*cis*-retinal in adjacent retinal pigment epithelial (RPE) cells is a fundamental process that allows regeneration of the vertebrate visual system. Here, we present evidence that *all-trans*-retinol is unstable in the presence of H^+ and rearranges to anhydroretinol through a carbocation intermediate, which can be trapped by alcohols to form *retro*-retinyl ethers. This ability of *all-trans*-retinol to form a carbocation could be relevant for isomerization. The calculated activation energy of isomerization of *all-trans*-retinyl carbocation to the 11-*cis*-isomer was only ∼18 kcal/mol, as compared to ∼36 kcal/mol for *all-trans*-retinol. This activation energy is similar to ∼17 kcal/mol obtained experimentally for the isomerization reaction in RPE microsomes. Mass spectrometric (MS) analysis of isotopically labeled retinoids showed that isomerization proceeds via alkyl cleavage mechanism, but the product of isomerization depended on the specificity of the retinoid-binding protein(s) as evidenced by the production of 13-*cis*-retinol in the presence of cellular retinoid-binding protein (CRBP). To test the influence of an electron-withdrawing group on the polyene chain, which would inhibit carbocation formation, 11-fluoro-*all-trans*-retinol was used in the isomerization assay and was shown to be inactive. Together, these results strengthen the idea that the isomerization reaction is driven by mass action and may occur via carbocation intermediate.

In the rod and cone photoreceptors, rhodopsin or cone visual pigments consist of the chromophore, 11-*cis*-retinal, coupled to the apoprotein (opsin, cone opsin) via protonated Schiff base (reviewed in ref *1*). Upon photoisomerization of 11-*cis*-retinal to *all-trans*-retinal (Figure 1, reaction 1), the chromophore transiently activates opsins, leading to G-protein signal transduction (*2*−*5*), and is ultimately released from the binding site. The removal of *all-trans*-retinal may be facilitated by an ATP-dependent transporter (ABCR) (*6*−*8*), but passive diffusion of the retinal is most likely sufficient (*9*). In the rate-limiting step in the retinoid cycle (*10*−*11*), *all-trans*-retinal is reduced to *all-trans*-retinol by *all-trans*-retinol dehydrogenase (Figure 1, reaction 2 and reverse reaction 3) (*12*−*19*). *all-trans*-Retinol passively diffuses to the retinal pigment epithelial cells (RPE)[1] (*20*) in a process most likely driven by trapping retinoids as insoluble fatty acid retinyl esters in RPE (*21*). The esterification reaction involves the transfer of an acyl group from the *sn*1 position of lecithin to retinol and is catalyzed by lecithin:retinol acyltransferase (LRAT; Figure 1, reaction 4) (*22*−*26*). Deigner et al. (*27*) proposed that these esters are substrates for an as yet unknown enzyme termed isomerohydrolase, which couples hydrolysis of the ester to the isomerization to 11-*cis*-retinol (Figure 1, reaction 6), thus providing the necessary energy to drive the reaction forward. Another alternative pathway involves the separation of these two reactions. The ester is first hydrolyzed by a retinyl hydrolase (Figure 1, reaction 5, reverse reaction 4) (*28*, *29*) and then isomerized to 11-*cis*-retinol directly or through some intermediate (Figure 1, reaction 7). This reaction would be driven by the use of retinoid-binding proteins and mass action (*30*−*33*). 11-*cis*-Retinol is then oxidized to 11-*cis*-retinal in a reaction catalyzed by NAD- and NADP-dependent 11-*cis*-retinol dehydrogenases (Figure 1, reaction 8, reverse reaction 9) (*14*, *34*−*39*). Finally, 11-*cis*-retinal diffuses to the rod photoreceptors, where it regenerates visual pigments (Figure 1).

The production of 11-*cis*-retinal is a fundamental process that allows regeneration of the visual system (*40*). The inhibition of 11-*cis*-retinal regeneration leads to severe

† This research was supported by the NIH vision training grant (J.K.M.), NIH Grants EY09339 (K.P.), Ruth and Milton Steinbach Fund, an MEC Grant SAF98-0143 (A.R.L.), and the E. K. Bishop Foundation.

* To whom correspondence should be addressed. Krzysztof Palczewski, Ph.D., University of Washington School of Medicine, Department of Ophthalmology, Box 356485, Seattle, WA 98195-6485. Phone: 206-543-9074; fax: 206-221-6784; e-mail: palczews@u.washington.edu.

‡ Department of Ophthalmology.

|| Department of Chemistry.

⊥ Department of Pharmacology.

§ Universidade de Vigo.

[1] Abbreviations: CRALBP, cellular retinaldehyde-binding protein; CRBP, cellular retinoid-binding protein; MS, mass spectrometry; RPE, retinal pigment epithelial cells.

10.1021/bi001061c CCC: $19.00
Published on Web 08/22/2000

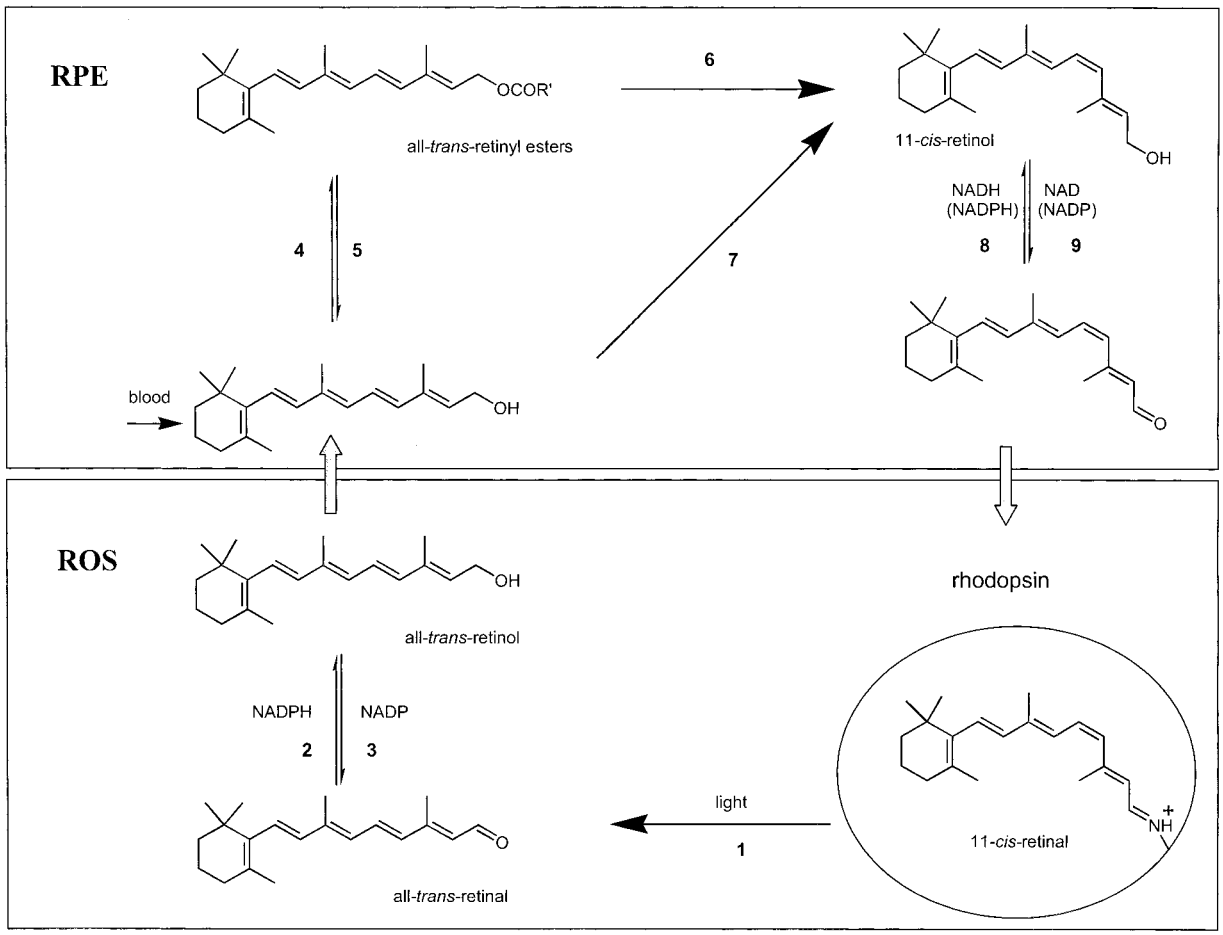

FIGURE 1: Retinoid cycle in the mammalian retina (see text for details).

impairment of vision. For example, a form of Leber congenital amaurosis is caused by mutations in a key protein of RPE, RPE65 (*41*−*43*). The phenotype of this disease is manifested as a lack of enzymatic production of 11-*cis*-retinal, leading to retina degeneration and ultimately blindness.

A full understanding of the retinoid cycle (also called the visual cycle) at the molecular level has not yet been accomplished, and the key isomerization reaction needs further characterization. Isomerization has been shown to occur enzymatically without an exogenous source of energy, and it was proposed that hydrolysis of *all-trans*-retinyl carboxylic esters would provide the energy needed for isomerization (∼4 kcal/mol) in a reaction catalyzed by a novel enzyme called isomerohydrolase (*27*). In this mechanism of isomerization, double bond migration and expulsion of the carboxylic group occur during the addition of a nucleophile to C_{11} of the retinyl ester. Low energy rotation about the $C_{11}-C_{12}$ single bond is followed by attack of water at C_{15} and concomitant reshuffling of the double bonds. The retinol becomes locked in the 11-*cis*-configuration, and the nucleophilic group is removed (*27*). An alternative mechanism, which involves apo-cellular retinaldehyde-binding protein (apo-rCRALBP), has been proposed recently. CRALBP enhances (*30*) or is necessary for efficient production of 11-*cis*-retinol in vitro (*31*−*33*) and in vivo (*44*). This process drives the reaction by mass action, overcoming the thermodynamically unfavorable isomerization. In previous studies, we have also shown that most of the ester pool does not participate in isomerization, which in turn suggests that a retinoid intermediate other than *all-trans*-retinyl ester is on the isomerization reaction pathway (*31*).

In this study, using chemical and enzymatic methods, we examined the mechanisms of 11-*cis*-retinol production in bovine RPE microsomes. First, we probed the behavior of *all-trans*-retinol and *all-trans*-retinyl palmitate to H^+ and base treatment and identified that *all-trans*-retinol is unstable in the presence of H^+ and readily forms a transient carbocation intermediate before it rearranges to anhydroretinol. In contrast, *all-trans*-retinyl palmitate reshuffles largely to the more thermodynamically stable *retro*-retinyl palmitate. This suggested that a carbocation could be also relevant for the isomerization reaction. Using quantum-mechanical calculations, the activation energy required for transition between *trans*−*cis* configurations was found to decrease from ∼36 kcal/mol for *all-trans*-retinol to ∼18 kcal/mol for the *all-trans*-retinyl carbocation. Experimentally, we found that the measured Arrhenius activation energy in vitro for *trans*−*cis* conversion also was in a range of 17−25 kcal/mol. Additionally, if the isomerization occurs through the addition of a nucleophile to C_{11} of the retinyl ester (*27*), it should be insensitive to the specificity of retinoid-binding proteins and would produce exclusively 11-*cis*-retinol. However, we provide evidence that this enzymatic reaction is highly dependent on the specificity of the retinoid-binding proteins and that other *cis*-isomers can readily be produced in the presence of alternative retinoid-binding proteins. This observation is in agreement with a carbocation as the interme-

diate of the isomerization reaction. Finally, we tested 11-fluoro-*all-trans*-retinol in the isomerization reaction. The addition of an electron-withdrawing constituent to the polyene chain makes the molecule more resistant to carbocation formation. As a consequence, this analogue is totally inactive in the enzymatic assay. Together, these data further strengthen the idea that the isomerization reaction is driven by mass action and may occur via a carbocation intermediate.

MATERIALS AND METHODS

Materials. Fresh bovine eyes were obtained from a local slaughterhouse (Schenk Packing Co., Inc, Stanwood, WA). Preparation of bovine RPE microsomes was described previously (*31*). The microsomes were resuspended in 10 mM 3-[N-morpholino]propanesulfonic acid (MOPS), 1 μM leupeptin, and 1 mM DTT to a total protein concentration of ~5 mg/mL as determined colorimetrically (*45*). Aliquots were stored at −80 °C and were used within 1 month of preparation. To destroy endogenous retinoids, 200-μL aliquots of RPE microsomes were irradiated in a quartz cuvette for 5 min at 0 °C using a ChromatoUVE-transilluminator (model TM-15 from UVP Inc.). All experiments were carried out under dim red light conditions.

Retinoid Preparations. All retinoids were freshly purified by normal phase HPLC (see conditions below, 10% ethyl acetate/hexane; detection at 325 nm). Purified *all-trans*-retinol was distributed in 0.5-nmol aliquots to 1.5-mL polypropylene tubes, dried under a stream of argon, and stored at −80 °C or redissolved in DMF to a concentration of 4 mM and stored at −80 °C. Retinoid concentrations in EtOH were determined spectrophotometrically: *all-trans*-retinal using $\epsilon = 42\,880$ M^{-1} cm^{-1} at 383 nm; *all-trans*-retinol using $\epsilon = 51\,770$ M^{-1} cm^{-1} at 325 nm (*46*).

Synthesis of Isotopically Labeled and Fluoro-Retinoids. [15-^{2}H,^{18}O]-*all-trans*-Retinol was synthesized from *all-trans*-retinal (Sigma) (Figure 2). *all-trans*-Retinal (1 μmol) was dissolved in 300 μL of a $CH_3CN/H_2{}^{18}O$ mixture at a ratio of 3:1. To accelerate the exchange of ^{16}O on *all-trans*-retinal, *p*-toluenesulfonic acid (2 mg) was added, and the mixture was incubated overnight at room temperature. An excess of $NaBD_4$ (~5 mg) was then added, and the reaction mixture was allowed to stand on ice for 20 min. The retinoids were extracted with 500 μL of hexane and purified by normal phase HPLC (HP1100; Beckman Ultrasphere Si 5μ, 4.6 × 250 mm; 10% ethyl acetate in hexane; flow rate 1.4 mL/min). Concentrations of retinoids were determined spectrophotometrically, and the extent of exchange was determined by MS.

[15-^{2}H,^{18}O]-*all-trans*-Retinyl palmitate (Figure 2) was synthesized by adding a 2-fold excess of palmitoyl chloride to a solution of [15-^{2}H,^{18}O]-*all-trans*-retinol and a 2-fold excess of triethylamine in anhydrous CH_2Cl_2. The reaction was kept at 0 °C for 12 h, washed with water, brine, and dried over $MgSO_4$. The organic layer was dried under a stream of argon, and the crude product was redissolved in hexane and purified by HPLC (as described above using 4% ethyl acetate/hexane). [15-^{2}H,^{18}O]-*all-trans*-Retinyl palmitate was collected, and the concentration was determined spectrophotometrically using $\epsilon = 51\,770$ M^{-1} cm^{-1} at 325 nm.

11-Fluoro-11-*cis*-retinal and 11-fluoro-*all-trans*-retinal were synthesized according to the protocol of Francesch et al. (*47*).

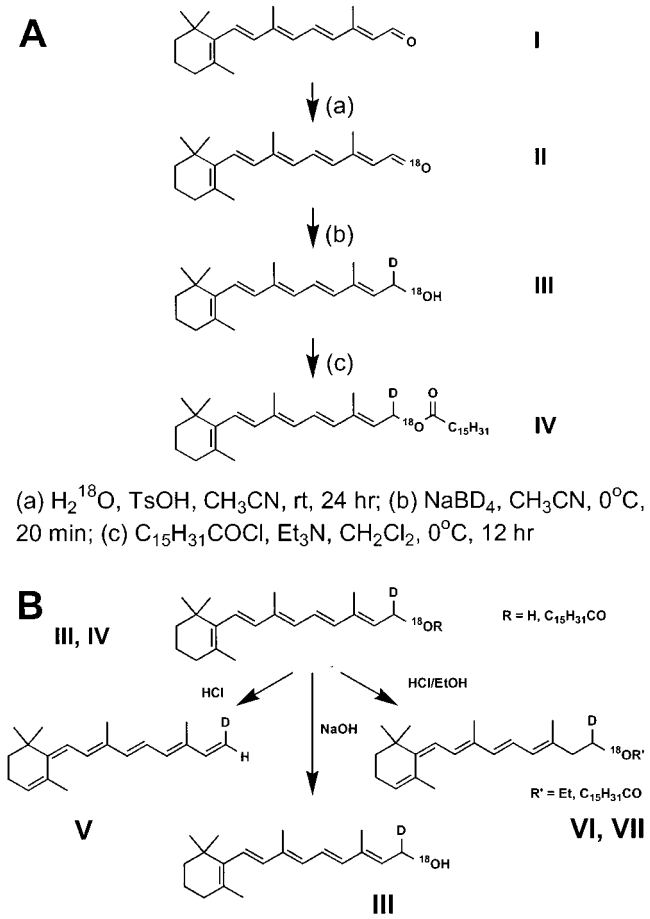

FIGURE 2: Schemes for synthesis of [15-^{2}H,^{18}O]-*all-trans*-retinol and [15-^{2}H,^{18}O]-retinyl palmitate and stability of these compounds to H^+ and base. (A) [15-^{2}H,^{18}O]-*all-trans*-Retinol was synthesized by, first, exchanging ^{16}O of *all-trans*-retinal with $H_2{}^{18}O$ (3:1 $CH_3CN/H_2{}^{18}O$) in the presence of *para*-toluenesulfonic acid. [^{18}O]-*all-trans*-Retinal was reduced with $NaBD_4$. [15-^{2}H,^{18}O]-*all-trans*-Retinyl palmitate was synthesized from [15-^{2}H,^{18}O]-*all-trans*-retinol and palmitoyl chloride. The products were purified by normal phase HPLC as described in Materials and Methods. (B) [15-^{2}H,^{18}O]-*all-trans*-Retinol or [15-^{2}H,^{18}O]-retinyl palmitate (in 90% CH_3CN) was subjected to 0.1 M HCl or 0.1 M HCl plus 10% EtOH for 30 min at 37 °C or by 0.1 M NaOH for 4 h at 37 °C.

These aldehydes were then reduced to the alcohols with $NaBH_4$ as described above.

Chemical and Spectrometric Analysis of Retinoids. To a solution of [15-^{2}H,^{18}O]-*all-trans*-retinol or [15-^{2}H,^{18}O]-*all-trans*-retinyl palmitate in 900 μL of CH_3CN, 100 μL of 1 M HCl or NaOH was added. The mixture was incubated for 30 min (HCl) or 4 h (NaOH) at 37 °C. The retinoids were extracted with 3 × 200 μL hexane, dried to a total volume of 100 μL under a stream of argon, and analyzed by HPLC (same conditions as above except 100% hexane for 5 min, 4% ethyl acetate/hexane for 15 min, then 10% ethyl acetate in hexane for 10 min). The retinoids were collected and analyzed by MS using a Kratos profile HV-3 direct probe mass spectrometer or a JEOL HX-110 direct probe mass spectrometer. The above experiment was then repeated with the addition of 100 μL of EtOH under identical conditions.

Cloning and Expression of CRBP in Escherichia coli. The coding sequence for the human CRBP type 1 was amplified from human Eye Cup cDNA library (obtained from Dr. Donald Zack, Johns Hopkins University) with primers FH410

(5′-GGATCCATGCCAGTCGACTTCACTG-3′) and FH411 (5′-GGTACCTCACTGCACCTTCTTGAATAC-3′) through 35 cycles at 94 °C for 30 s, 56 °C for 30 s, and 68 °C for 2 min. The PCR product was cloned in pCRII-TOPO vector (Invitrogen) and sequenced by dyedeoxyterminator sequencing (ABI-Prism, Perkin-Elmer). The coding sequence for CRBP1 was then transferred as a fragment *Bam*HI-*Kpn*I in the pQE30 expression vector (Qiagen, Chatsworth, CA) opened with *Bam*HI-*Kpn*I and fused to a 6 His-tag. The pQE30-CRBP1 plasmid was then transferred in *Escherichia coli* M15, and the expression of CRBP was induced by incubation for 5 h in the presence of 1 mM IPTG.

Preparation of Apo-Recombinant CRALBP and Apo-Recombinant CRBP. Recombinant CRBP and CRALBP were purified to homogeneity by Ni^{2+}-affinity chromatography as described by Crabb et al. (*48*).

Reaction Conditions for Isomerase and LRAT Reaction. Retinoids were delivered either by the dry method (*31*−*33*) or by the addition of 0.5 μL of 4 mM *all-trans*-retinol or [15-^{2}H,^{18}O]-*all-trans*-retinol in DMF (2 nmol). DMF was found to be more effective in delivering retinoids into the assay than the dry method used previously (*33*). To a 1.5-mL polypropylene tube containing 2 nmol of [15-^{2}H,^{18}O]-*all-trans*-retinol, 20 μL of 10% BSA (in 10 mM BTP, pH 7.5) and 15−30 μL of apo-rCRALBP or CRBP (in 10 mM BTP, pH 7.5; final concentration ∼25 μM) were added. Next, 10 mM BTP, pH 7.5, containing 0.5 mM ATP was added to bring the total volume to 180 μL. Last, 20 μL of UV-treated bovine RPE microsomes (∼100 μg of protein) were added to the mixture. The reactions were incubated at 37 °C for the indicated times.

The above assay was used to determine the measured Arrhenius activation energy by varying the temperature of the incubation from 6 to 53 °C in 6° increments. The time course ranged from a maximum of 0−45 min in 15-min increments for lowest temperatures, and 0−15 min for highest in 5 min increments. Each measurement was performed in duplicate. Rates were determined from the amounts of 11-*cis*-retinol produced. The initial rate was calculated by performing a linear regression over only those points that fit the initial rate well (typically 2 or 3) or from a linear regression across all points measured for the time course. An Arrhenius plot was created, and a linear regression was performed on all temperatures except 47 and 53 °C, where the isomerase showed a decrease in overall rate. Both methods of initial rate calculations gave similar activation energies.

MS Analysis of Retinoids Produced in RPE Microsomes in the Presence of Apo-Recombinant CRALBP. To generate substantial amounts of retinoids for MS analysis, 60 samples of the above reaction mixtures were incubated simultaneously for 2 h in the presence of recombinant apo-CRALBP. The vials were centrifuged at 112000*g* for 30 min at 4 °C to pellet the microsomes. The supernatant was then transferred to new vials and quenched with 300 μL of MeOH and 300 μL of hexane. The mixture was vortexed for 2 min and centrifuged at 14 000 rpm for 4 min to separate the phases. This extraction was repeated, and the hexane fractions were pooled and dried down under a stream of argon. The crude product was redissolved in 300 μL of hexane and was centrifuged at 14 000 rpm to remove any insoluble particles. The hexane extract was loaded in 100-μL fractions onto HPLC (10% ethyl acetate/hexane). Fractions containing 11-*cis*-retinol and *all-trans*-retinol were collected, pooled, and dried down under a stream of argon. The 11-*cis*-retinol and *all-trans*-retinol were rechromatographed in 4% ethyl acetate/hexane and analyzed by MS and tandem MS-MS using a JEOL HX-110 mass spectrometer.

MS Analysis of Retinoids Produced in RPE Microsomes in the Presence of Apo-Recombinant CRBP Type I. Approximately 100 isomerization assay vials were incubated for 1 h at 37 °C in the absence of retinoid-binding proteins. Then 25 μM CRBP (final concentration) in 10 mM BTP, pH 7.5, was added to each vial, and the sample was incubated for an additional 2 h. The samples were then processed and purified as described above. MS analysis was performed using a Kratos profile HV-3 direct probe mass spectrometer. For 13-*cis*-retinol (Figure 7, panel E), the results were obtained by performing a plot of peak intensity versus time for the fragments characteristic of retinoids (289, 287, 269, 255) and then performing a background subtraction against a point of low intensity for these ions. This was done to eliminate interference from a contaminant that coeluted with the 13-*cis*-retinol. All other spectra received no manipulation.

Quantum-Chemical Calculations. Quantum-chemical calculations were performed using the Gaussian-98 suite of programs (Gaussian, Inc., Pittsburgh, PA). The semiempirical AM1 approximation was initially used because of its less demanding computational requirements. The more reliable ab initio methods of Hartree−Fock (HF) and density-functional B3LYP implementation were used for refinement. The 6-31g* basis set was used for both ab initio methods.

Geometry optimization was done in Cartesian coordinates with the default precision. The transition state for trans-cis rotation was modeled by the 90° constraint of the corresponding dihedral angle. The constraint was implemented as a redundant coordinate, and the reference zero-energy was taken to be the energy of the *trans*-isomer in all cases.

RESULTS

To follow chemical and enzymatic transformations, [15-^{2}H,^{18}O]-labeled *all-trans*-retinol and *all-trans*-retinyl palmitate were prepared (Figure 2). The exchange of ^{16}O to ^{18}O ranged between 50 and 90% in different preparations and was dependent on the ratio of *all-trans*-retinal to $H_2{}^{18}O$ and the time of the exchange reaction. The [^{18}O]-*all-trans*-retinal was then reduced with $NaBD_4$ to permit distinction of exogenously added [15-^{2}H]-*all-trans*-retinol from any residual *all-trans*-retinol endogenous to RPE. MS was used to analyze these stable isotope-labeled retinoids.

Stability of all-trans-Retinol and all-trans-Retinyl Palmitate to Acid and Base. [15-^{2}H,^{18}O]-*all-trans*-Retinol (∼50% ^{16}O to^{18}O exchange, peak 1, chromatogram a; Figure 3A) was treated with 0.1 M HCl for 30 min at 37 °C. The product of this reaction (peak 2 in chromatogram b, Figure 3B) produced UV spectra with maxima at 352, 368, and 388 nm, and MS analysis showed M^+ ion at 269 *m*/*z* (loss of $H_2{}^{18}O$ and $H_2{}^{16}O$) and a fragmentation ion of 254 *m*/*z* (loss of C^2-HH or CH_3) (Figure 3A). These data indicate that the product is anhydroretinol, most likely a mixture of geometric isomers (*49*). To test whether anhydroretinol formed via carbocation, H^+ treatment was carried out in the presence of EtOH. [15-^{2}H]-*all-trans-retro*-Retinyl ethyl ether was formed after ^{18}-

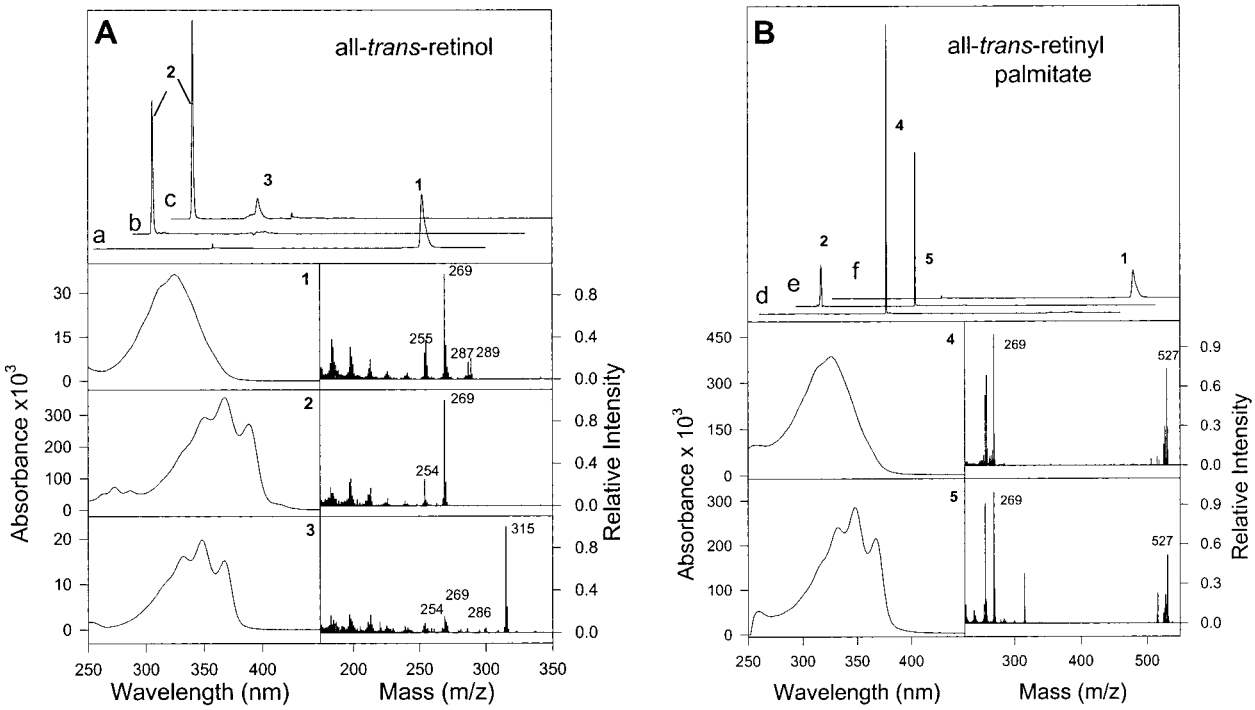

FIGURE 3: Influence of acid and base on *all-trans*-retinol and *all-trans*-retinyl palmitate. (A) Traces a, b and c, respectively, show HPLC chromatograms of untreated [15-^{2}H,^{18}O]-*all-trans*-retinol, retinol (in 90% CH_3CN) treated with 0.1 M HCl for 30 min at 37 °C, and retinol treated with 0.1 M HCl and 10% EtOH for 30 min at 37 °C. The peak **1** shows the characteristic UV−Vis (left panel) and MS (right panel) spectra of *all-trans*-retinol. Equal amounts of [15-^{2}H,^{16}O]-*all-trans*-retinol and [15-^{2}H,^{18}O]-*all-trans*-retinol were present. The peak **2** shows the product of H^+ degradation of [15-^{2}H,^{18}O]-*all-trans*-retinol with characteristic UV−Vis and MS spectra of [15-^{2}H]-anhydroretinol. Peak **3** shows characteristic UV−Vis and MS spectra of [15-^{2}H]-*all-trans-retro*-retinyl ethyl ether formed during H^+ elimination in the presence of EtOH. (B) Traces d, e, and f, respectively, show HPLC chromatograms of untreated [15-^{2}H,^{18}O]-*all-trans*-retinyl palmitate, the ester treated with 0.1 M HCl for 30 min at 37 °C in 90% CH_3CN, and the ester treated with 0.1 M NaOH for 4 h at 37 °C. Peak **4** shows UV−Vis spectrum (left panel) and MS fragmentation patterns (right panel) consistent with those of [15-^{2}H,^{18}O]-*all-trans*-retinyl palmitate. Peak **2** was analogous to peak **2** in panel A, and it has been identified as [15-^{2}H]-anhydroretinol. Peak **5** displays UV−Vis and MS spectra of [15-^{2}H,^{18}O]-*all-trans-retro*-retinyl palmitate. Finally, peak **1** represents the product of hydrolysis of [15-^{2}H,^{18}O]-*all-trans*-retinyl palmitate by NaOH to [15-^{2}H,^{18}O]-*all-trans*-retinol.

OH elimination in the presence of EtOH (chromatogram c, peak 3), producing a characteristic UV−vis spectrum (left panel) and a 315 *m*/*z* molecular mass ion with a fragmentation pattern (right panel) similar to that described earlier for a related compound (*50*). Furthermore, ^{18}O was lost during the reaction, suggesting that the carbocation was formed as an intermediate. [15-^{2}H,^{18}O]-*all-trans*-Retinol was stable in 0.1 M NaOH for 4 h at 37 °C (data not shown) and did not lose its ^{18}O-label.

[15-^{2}H,^{18}O]-*all-trans*-Retinyl palmitate (∼50% ^{16}O to^{18}O exchange, peak 4, chromatogram d; Figure 3B) was also sensitive to H^+ treatment and converted mostly to [15-^{2}H,^{18}O]-*all-trans-retro*-retinyl palmitate, an isomer of *all-trans*-retinyl palmitate, but with characteristic UV−Vis absorption maxima at 334, 348, and 368 nm (peak 5 in chromatogram e, Figure 3B). Anhydroretinol (peak 2, chromatogram e, Figure 3B), which formed as a minor product also during this reaction, could either be produced from the ester by H^+ hydrolysis and dehydration of *all-trans*-retinol or directly from [15-^{2}H,^{18}O]-*all-trans*-retinyl palmitate. The mechanism responsible for the formation of anhydroretinol from *all-trans*-retinyl palmitate was not resolved. [15-^{2}H,^{18}O]-*all-trans*-Retinyl palmitate hydrolyzed in 0.1 M NaOH through $B_{AC}1$ acyl cleavage mechanism (*51*) to yield [15-^{2}H,^{18}O]-*all-trans*-retinol (chromatogram f, Figure 3B, mass spectrum was similar to that of peak 1 in Figure 3A). These data together indicate that *all-trans*-retinol was unstable to H^+ treatment and rearranged to anhydroretinol via a carbocation intermediate; *all-trans*-retinyl palmitate was more stable than *all-trans*-retinol and converted mostly to *retro*-retinyl palmitate. Formation of a carbocation in the presence of an electrophilic agent appeared to be the more appropriate path of chemical transformation than nucleophilic addition to olefinic carbon. Next, we investigated whether a carbocation was an energetically favorable intermediate for the isomerization of *all-trans*-retinol to 11-*cis*-retinol.

Theoretical Calculations of the Transition State Energies for all-trans-Retinol to 11-cis-Retinol Isomerization. The free energy reaction coordinate profile for the transformation of *all-trans*-retinol to the 11-*cis*-isomer through a carbocation intermediate was calculated employing AM1, HF, and B3LYP methods (Materials and Methods). Transition state calculations showed that the isomerization of *all-trans*-retinol to 11-*cis*-retinol by rotation about the $C_{11}-C_{12}$ double bond without delocalization of electrons in the polyene chain required 36.2 kcal/mol (B3LYP). However, if the isomerization occurred through the *all-trans*-retinyl carbocation, where the positive charge is distributed along the polyene chain of the chromophore, it would require only 17.2 kcal/mol to rotate the $C_{11}-C_{12}$ bond from *trans*- to *cis*-conformation (Figure 4A).

While carbocation formation is an exothermic reaction that involves protonation of the hydroxy group and elimination of the water molecule, the reverse endothermic hydration of

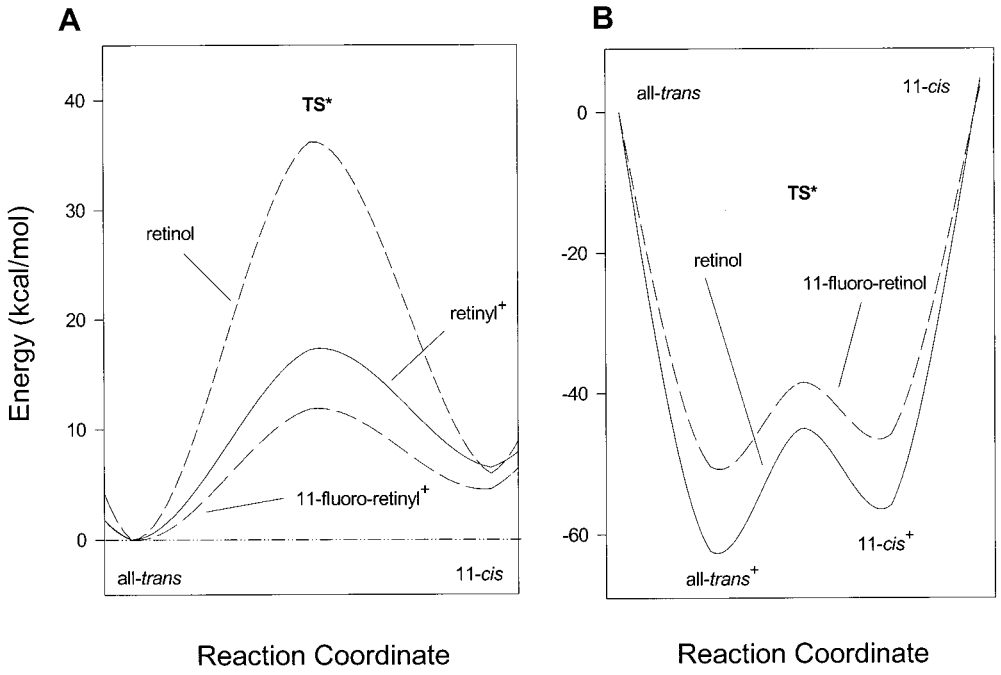

FIGURE 4: Theoretical calculations of the transition state energies of carbocation intermediates for *all-trans*-retinol and 11-fluoro-*all-trans*-retinol and comparison of the ground and transition state energies for *all-trans*-retinol, *all-trans*-retinyl, and 11-fluoro-*all-trans*-retinyl carbocation. Transition state for *trans*−*cis* rotation was modeled by the 90° constraint of the $C_{10}-C_{11}-C_{12}-C_{13}$ dihedral angle. Energy values shown on the graphs are calculated using the ab initio B3LYP method. The energy of *all-trans*-isomers was taken as reference zero energy. (A) Isomerization of *all-trans*-retinol without electron delocalization of the polyene chain requires overcoming an energetic barrier of 36.2 kcal/mol. With carbocation formation, this energy decreases to 17.2 kcal/mol. The activation energy of 11-fluoro-*all-trans*-retinyl carbocation is only 11.8 kcal/mol. (B) Free energy reaction coordinate profile for isomerization of *all-trans*-retinol and 11-fluoro-*all-trans*-retinol to their corresponding 11-*cis*-isomers through carbocation intermediates. For the carbocation to be formed, the *all-trans*-isomer is protonated with a hydroxonium ion. Exothermic dehydration of the protonated *all-trans*-isomer leads to the formation of *all-trans*-carbocation followed by endothermic *trans*−*cis* rotation (for values see above). The energy of endothermic hydration and deprotonation of 11-*cis*-retinyl and 11-fluoro-11-*cis*-retinyl carbocations is 1.7 and 0.9 kcal/mol (respectively) less than the energy of exothermic dehydration for formation of the carbocation. For structures refer to Figure 9.

the 11-*cis*-carbocation required 1.7 kcal/mol less energy. The conclusion of these calculations is that formation of the carbocation significantly lowers the activation energy of the transition state during the isomerization process. However, for the complex reaction in RPE microsomes, it was unknown how much energy would be needed for enzymatic isomerization.

Experimental Determination of the Activation Energy for the Isomerization Reaction in Bovine RPE Microsomes. To determine experimentally the activation energy of the enzymatic isomerization of *all-trans*-retinol to 11-*cis*-retinol in RPE microsomes, time courses of 11-*cis*-retinol production were performed at different temperatures, and the Arrhenius plot was calculated. The logarithm of the initial rates of reaction vs $1/T$ is shown in Figure 5. A linear least-squares fitting of the points from 5 to 41 °C was performed, and the slope was used to calculate the measured Arrhenius activation energy using the equation (eq 1):

$$\text{slope} = -E_a/2.303R \qquad (1)$$

where R is the gas constant (1.98 kcal/K mol), and E_a is the activation energy. The measured Arrhenius activation energy was calculated to be in a range of 17−25 kcal/mol and was in good agreement with the theoretical calculations. If isomerization occurs via carbocation, different geometrical isomers would be observed in the presence of retinoid-binding proteins with the appropriate specificity. However, if the mechanism involves a covalent intermediate as proposed previously (*27*), retinoid-binding proteins should not have any influence on which isomer is formed.

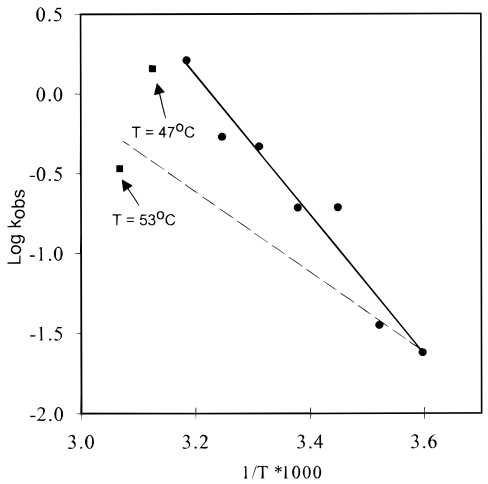

FIGURE 5: Arrhenius plot of isomerase activity in bovine RPE microsomes. The rate of formation of 11-*cis*-retinol was measured in duplicate at temperatures ranging from 5 to 53 °C in 6° increments. The log of the rate was plotted against $1/T$. A linear least-squares measurement was performed from 5 to 41 °C (47 and 53 °C were excluded because of temperature-dependent inactivation of enzymes of the visual cycle). The measured Arrhenius activation energy was calculated from the slope and was found to be in the 17 kcal/mol range (solid line). The dashed line represents a typical enzymatic reaction when the rate doubles every 10 °C.

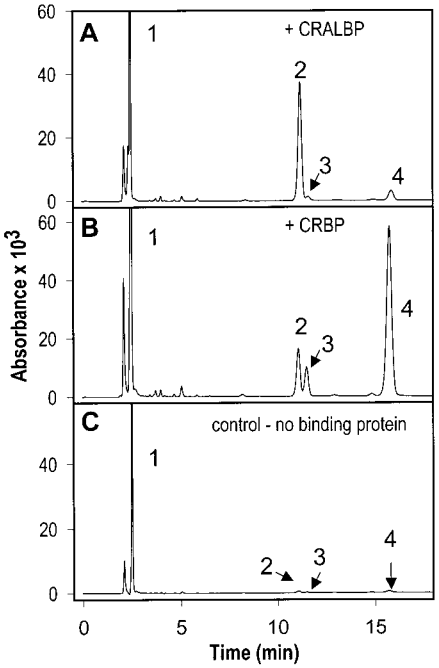

FIGURE 6: Influence of retinoid-binding proteins on the formation of different retinol isomers. Panels A and B show chromatograms of the formation of retinol isomers in the presence of CRALBP and CRBP, respectively. The peaks were identified as follows: **1**, retinyl esters; **2**, 11-*cis*-retinol; **3**, 13-*cis*-retinol, and **4**, *all-trans*-retinol. A control experiment without retinoid-binding proteins, panel C, shows the near absence of *cis*-retinols, while *all-trans*-retinol was almost completely esterified.

Comparison of the Effects of Different Retinoid-Binding Proteins in the Isomerization Assay. To compare the effects of retinoid-binding proteins on isomerization, RPE microsomes were incubated for 1 h at 37 °C with [15-^{2}H,^{18}O]-*all-trans*-retinol. Next, retinoid-binding protein (~25 μM final concentration) was added and incubated for an additional 2 h. Figure 6 shows that in the absence of retinoid-binding protein, the added *all-trans*-retinol was completely converted to retinyl esters (Figure 6, panel C), showing only traces of other retinoids. With the addition of retinoid-binding protein, however, isomers of *all-trans*-retinol were produced, with CRALBP promoting almost exclusively 11-*cis*-retinol production (Figure 6, panel A). The small amount of 13-*cis*-retinol is likely a result of spontaneous thermal isomerization. The addition of CRBP to the reaction produced primarily *all-trans*-retinol but to a lesser extent 11-*cis*-retinol and 13-*cis*-retinol, the latter in an amount that could not be explained by spontaneous thermal isomerization. MS analysis was necessary to determine whether 13-*cis*-retinol had formed enzymatically or spontaneously. If 13-*cis*-retinol was formed via a carbocation intermediate from [15-^{2}H,^{18}O]-*all-trans*-retinol, it would lose the ^{18}O label, while if it is formed spontaneously, the label would be retained.

MS Analysis of Retinoid Isomers Generated in Isomerase Assays. To better understand the mechanism by which *cis*-retinol is formed, the isotope composition of retinols produced from [15-^{2}H,^{18}O]-*all-trans*-retinol was analyzed. Using direct probe MS, the analysis of standard *all-trans*-retinol showed a fragmentation pattern of 286 (M^+), 268 ($-H_2O$), and 255 ($-CH_2OH$) (Figure 7, panel A). The synthesized [15-^{2}H,^{18}O]-*all-trans*-retinol, with a typical yield of 80−90%, showed predominantly 289 (M^+) peak. 11-*cis*-

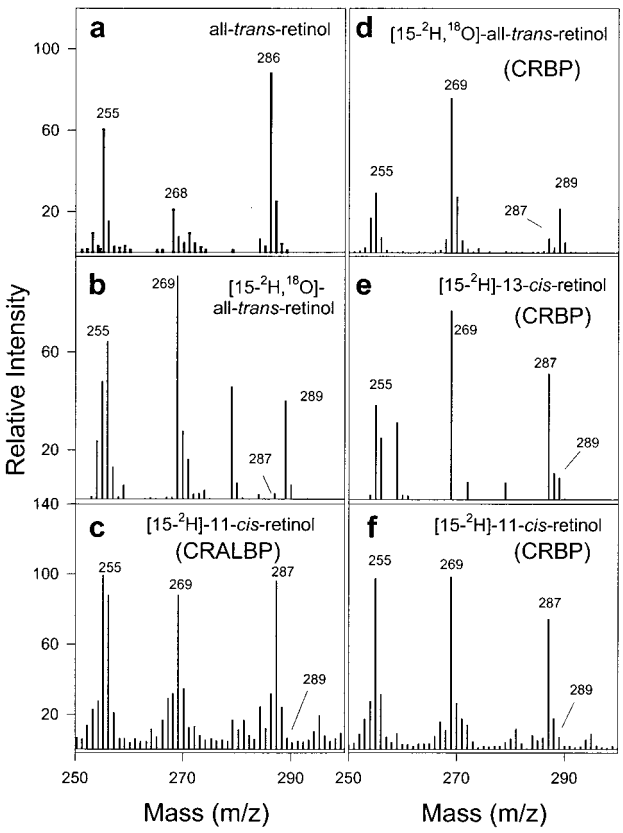

FIGURE 7: MS analysis of *cis*-retinols formed from [15-^{2}H,^{18}O]-*all-trans*-retinol in the presence of different retinoid-binding proteins in RPE microsomes. Panel a shows the MS fragmentation pattern of standard *all-trans*-retinol, and panel b shows the fragmentation pattern of the synthesized [15-^{2}H,^{18}O]-*all-trans*-retinol. Note the shift from 286 to 289 because the presence of ^{2}H and ^{18}O and a fragment at 269 due to ^{2}H. Panel c shows a loss of ^{18}O upon the formation of 11-*cis*-retinol when CRALBP was used as a retinoid-binding protein. Panel d shows that *all-trans*-retinol bound to CRBP retains the ^{18}O-label, yet panels e and f show that 13-*cis*-retinol and 11-*cis*-retinol formed in the presence CRBP lost ^{18}O. Note that the deuterium label is retained in each measurement.

Retinol generated in the presence of CRALBP (Figure 6, panel A) showed loss of ^{18}O-label (Figure 7, panel C). Deigner et al. (*27*) have made similar observations for this reaction in the absence of retinoid-binding proteins. However, [15-^{2}H,^{18}O]-*all-trans*-retinol bound to CRBP (Figure 7, panel D) retained ^{18}O and was most likely generated by hydrolysis of *all-trans*-retinyl esters (*29*). More importantly, 13-*cis*-retinol and 11-*cis*-retinol bound to CRBP (Figure 7, panels E and F) showed ^{18}O exchange.

Lack of Isomerization of 11-Fluoro-all-trans-retinol by RPE Microsomes. The formation of a carbocation could be a critical step in the isomerization reaction. Therefore, it was interesting to study the influence of substituents on the polyene chain. For this purpose, 11-fluoro-*all-trans*-retinol was chosen. The presence of a strong electron-withdrawing group changes the electronic properties of *all-trans*-retinol. The addition of fluorine would increase the positive charge delocalized across the polyene chain, making the molecule more resistant to protonation. Quantum-mechanical calculations determined that isomerization of 11-fluoro-retinyl carbocation to its 11-*cis*-isomer proceeds through a smaller energetic barrier of only 11.8 kcal/mol as compared to *all-trans*-retinyl carbocation (17.2 kcal/mol) (Figure 4). Fur-

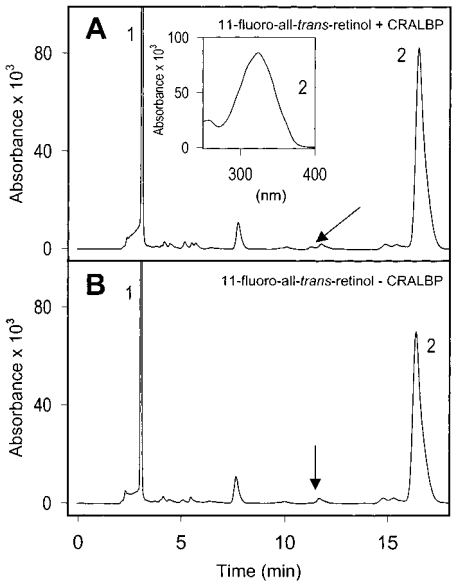

FIGURE 8: Lack of isomerization of 11-fluoro-*all-trans*-retinol by RPE microsomes. The isomerization reaction for 11-fluoro-*all-trans*-retinol (0.5 nmol) was carried out as described in Materials and Methods with (A) and without (B) 25 μM CRALBP. The arrows point to the expected elution time of 11-fluoro-11-*cis*-retinol. Note that only a small amount of 11-fluoro-11-*cis*-retinol is formed, most likely nonenzymatically.

thermore, the total charge across the polyene chain of the 11-fluoro-retinyl carbocation was calculated to be +1.34e, while the charge of the *all-trans*-retinyl carbocation was found to be +0.75e. Thus, the presence of fluorine increased the positive charge by 0.58e. This calculation explains why 11-fluoro-*all-trans*-retinol formed 11-fluoro-anhydroretinol ~5 times slower during H^+ treatment than the rate of *all-trans*-retinol conversion to anhydroretinol (data not shown). For native *all-trans*-retinol, the charge on C_{11} was found to be −0.12e, while in the 11-fluoro-*all-trans*-retinol it was +0.11e, suggesting that if the isomerization occurs via covalent intermediate (*27*), the enzyme derivative should be formed more readily with the fluorinated retinol.

Substitution of the C_{11} proton of *all-trans*-retinol with fluorine resulted in a lack of 11-fluoro-11-*cis*-retinol formation regardless of the presence of CRALBP in the isomerization assay (Figure 8). In both cases, a small amount of 11-fluoro-13-*cis*-retinol was present but likely due to spontaneous thermal isomerization. However, the failure of 11-fluoro-*all-trans*-retinol to isomerize was not due to the inability of 11-fluoro-11-*cis*-retinol to bind to CRALBP. Using previously published assays (*32*), 11-fluoro-11-*cis*-retinol showed only ~20% less affinity for CRALBP than 11-*cis*-retinol (data not shown). 11-Fluoro-11-*cis*-retinol was stable in these conditions and did not isomerize spontaneously to the *all-trans*-isomer. In addition, the ability of LRAT to readily esterify 11-fluoro retinol suggested that lack of isomerization was not due to poor enzymatic property of this enzyme. We cannot rule out, however, that the fluorine atom inversely affects isomerization by other mechanisms.

DISCUSSION

Photoreceptors utilize the photoisomerization reaction of 11-*cis*-retinal to *all-trans*-retinal to trigger phototransduction, which subsequently results in the sensation of vision. Regeneration of 11-*cis*-retinal occurs in adjacent RPE cells and is anchored by the isomerization of *all-trans*-retinol (or *all-trans*-retinyl esters) to 11-*cis*-retinol. To explore this process, we used chemical approaches in combination with enzymatic assays using retinoids labeled with stable isotopes, bovine RPE microsomes, and retinoid-binding proteins. Significant data and additional insight have been obtained leading to a proposal of a novel mechanism of isomerization that may occur through a carbocation intermediate.

Nucleophilic Addition to C_{11} versus Carbocation Formation. Deigner et al. (*27*) first proposed a mechanism for the isomerization of *all-trans*-retinol to 11-*cis*-retinol. Under this proposal, an enzyme termed isomerohydrolase utilizes the energy of hydrolysis of the retinyl ester to rotate the C_{11}−C_{12} bond of *all-trans*-retinol. The proposed mechanism by which this double bond is transformed to a single bond assumes nucleophilic addition to C_{11} and reshuffling of double bonds followed by elimination of the carboxylate group from the ester. This proposed mechanism presents several conceptual dilemmas (*31*, *32*) such as (i) addition of nucleophile to an electron-rich olefinic chain; (ii) the breaking of double bond conjugation, and (iii) addition of water to an anhydroretinol-like structure to restore 11-*cis*-retinol. According to this hypothesis, isomers other than 11-*cis*-retinol cannot be produced, a prediction that is inconsistent with our experimental data. Formation of 13-*cis*-retinol would be only allowed if addition of water molecule would not be restricted in space and would occur on two substrate intermediates in 11-*cis* and 13-*cis* configuration. This is an unlikely proposition for an enzymatic reaction. Furthermore, an increase in the positive charge of 0.23e at the C_{11} position in 11-fluoro-*all-trans*-retinol did not enhance production of the 11-*cis*-isomer, which would most likely occur if isomerization occurred by nucleophilic attack. However, this analogue was ineffective in the isomerization reaction.

There is ample evidence for the existence of a carbocation intermediate as a transition state for retinoids. Earlier studies involving pump−probe spectroscopy using *all-trans*-retinyl acetate have shown that carbocations can exist under certain chemical conditions for up to 5−10 ns (*52*). The formation of anhydroretinol isomers from *all-trans*-retinol in the presence of H^+ also indicates that protonation leads to the elimination of water and a loss of bond-order along the polyene chain (*49*). This water loss has been further supported by the addition of EtOH to a solution of [15-^{2}H,^{18}O]-*all-trans*-retinol in the presence of H^+. The compound created, *all-trans-retro*-retinyl ethyl ether could only be formed by the reaction of a carbocation produced from *all-trans*-retinol and EtOH as indicated by the 315 M^+ peak (panel 3, Figure 3A). Finally, the fact that *all-trans*-retinyl palmitate hydrolyzed back to retinol in basic conditions without losing ^{18}O label and that it rearranged mostly to *all-trans-retro*-retinyl palmitate under acidic conditions suggests that *all-trans*-retinol forms a carbocation intermediate under similar conditions more readily. The presence of a strong electron-withdrawing group, fluorine, caused an increase in the positive charge of the polyene chain by 0.58e. This significantly increases electrostatic repulsion between the retinyl chain and the proton-donating group of the putative enzyme and would inhibit isomerization. Thus, the protonation reaction—the first step in the formation of a carbocation transition state—would be more difficult. This was

confirmed by showing that 11-fluoro-*all-trans*-retinol was significantly more stable than *all-trans*-retinol in the presence of H^+ and did not undergo isomerization in the enzymatic tests.

Activation Energy and the Thermodynamic Equilibrium of trans-cis-Isomerization. To shed light on the energy flow during the *trans*−*cis* isomerization reaction, we employed quantum-mechanical methods to calculate energy profiles for the transition state intermediates. For isomerization to occur without delocalization of electrons in the polyene chain, it must overcome an energetic barrier of 36.2 kcal/mol, and two conjugated radicals would represent a transition state. For the isomerization of the *all-trans*-retinyl carbocation formed by dehydration of *all-trans*-retinol, however, E_a is significantly lower at 17.2 kcal/mol. This value closely matches the experimentally apparent $E_a = 17-25$ kcal/mol for the isomerization process using the Arrhenius equation (Figure 5).

The exothermic effect of carbocation formation (Figure 4) can be explained by the favorable distribution of positive charge through electron delocalization across the polyene chain, thus reducing the bond order (Figure 9). The energy released by this process is likely stored by the enzyme, possibly as an unfavorable conformational change. As equilibrium between *trans*−*cis* carbocations is established, the reaction is completed by hydration of the *cis*-retinyl carbocation, which is an endothermic process and takes 1.7 kcal/mol less energy than was produced during protonation. The formation of a carbocation makes isomerization kinetically feasible. However, to overcome the thermodynamic free energy difference of 4.7 kcal/mol between the *all-trans*-retinol and 11-*cis*-retinol ground states, retinoid-binding proteins are necessary to drive the reaction forward.

Our mechanism explains the necessity of retinoid-binding protein for efficient isomerization, which does not occur to appreciable levels without withdrawal of the *cis*-isomers, despite favorable energies (1 kcal/mol) for the isomerohydrolase reaction (*53*). Previous interpretation of this fact (*28*) assumes potent inhibition by the formed product of the isomerization reaction. However, the inhibition IC_{50} ~400 nM is well above the concentration of membrane-soluble 11-*cis*-retinol in our system (*31*−*33*). Furthermore, in 11-*cis*-retinol dehydrogenase knockout mice, high concentrations of 11-*cis*- and 13-*cis*-retinol, and 11-*cis*- and 13-*cis*-retinyl esters were observed even though the production of 11-*cis*-retinal was unaffected (*36*). Thus, in vivo inhibition of 11-*cis*-retinol production by *cis*-retinoids was not observed. These two reasons suggest that inhibition of isomerization by *cis*-retinoid products is of minor consideration.

Specificities of Retinoid-Binding Proteins: How Could They Influence the Isomerization Process? The use of stable-isotope labeled retinoids and MS analysis provided an excellent method to study the mechanistic process of the isomerization reaction. This technique had been used earlier to study isomerization (*27*); however, in the current study it has been expanded to include not only additional binding proteins but also the inclusion of deuterium at the C_{15} position to distinguish exogenous retinols from endogenous retinols. The use of the ^{18}O label on [15-^2H,^{18}O]-*all-trans*-retinol would enable us to determine an important issue in the esterification/hydrolysis/isomerization pathway: Is the ^{18}O label lost during the esterification process or during isomerization (i.e., does esterification/isomerization operate by alkyl cleavage or acyl cleavage)?

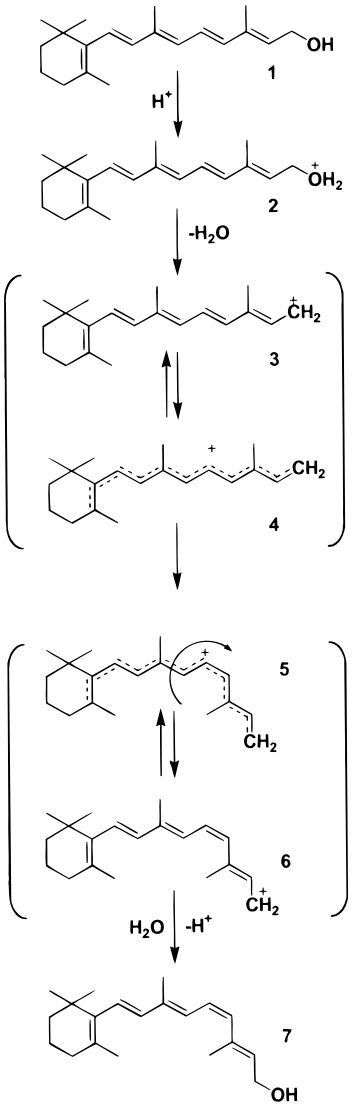

FIGURE 9: Proposed chemical mechanism for the formation of 11-*cis*-retinol via carbocation intermediate by the isomerization reaction in mammalian RPE microsomes (see text for details).

Previous studies (*31*) had shown that when using CRBP as a binding-protein, 11-*cis*-retinol and *all-trans*-retinol were produced. For this reason, it was necessary to pre-esterify exogenously added [15-^2H,^{18}O]-*all-trans*-retinol before the addition of binding proteins to distinguish *all-trans*-retinol bound to CRBP as a result of ester hydrolysis, from the exogenously added *all-trans*-retinol. Additionally, with the use of better chromatographic separation, it was discovered that 13-*cis*-retinol is produced in quantities greater than can be explained by spontaneous thermal isomerization when using CRBP. This result is contrary to the proposed isomerohydrolase mechanism that would favor formation of a single isomer, 11-*cis*-retinol.

The MS analysis showed that *all-trans*-retinol bound to CRBP retained the ^{18}O-label (Figure 7, panel D), while it was clearly lost on 11-*cis*-retinol and 13-*cis*-retinol isomers (Figure 7, panels E and F). The fact that *all-trans*-retinol bound to CRBP retained the ^{18}O label strongly indicates that LRAT/hydrolase operates via acyl cleavage mechanism, and

both enzymes establish rapid equilibrium of free *all-trans*-retinol. Additionally, the loss of ^{18}O by 11-*cis*-retinol and 13-*cis*-retinol bound to CRBP demonstrates that isomerization involves alkyl cleavage mechanism and possibly a carbocation intermediate.

How these retinoid-binding proteins influence the isomerization process is unclear and requires more experiments. It appears that once different carbocation isomers are produced, they are hydrated and are released by the isomerase. The retinoid isomers are quickly picked up by the retinoid-binding protein and removed to solution. Thus, the rate at which a particular retinoid isomer is formed merely depends on its particular specificity for the retinoid-binding protein present. In the case of CRALBP, the production of only the 11-*cis*-isomer formed by the isomerase is accelerated relative to the other isomers because of its high affinity and specificity of this protein. CRBP's preference for *all-trans*-retinol leads to rapid hydrolysis of *all-trans*-retinyl esters. However, the 11-*cis*-retinol and 13-*cis*-retinol production is accelerated because CRBP also demonstrates specificity for these two isomers (*54*). It appears that the isomerase is not specific to 13- and 11-*cis*-isomer, merely making retinoid isomers as determined solely by thermodynamic equilibrium. The deciding factor that determines which isomer is produced is the specificity of the retinoid-binding protein, and the accumulation of particular isomers will be accelerated.

Carbocations in Biology. Reactions via carbocation intermediates are not uncommon in biology. A number of recently studied mechanisms have been suggested to operate by a carbocation intermediate. Some examples include the cyclization of farnesyl diphosphate to pentalenene (*55*) and the cyclization of the β-, ϵ-, and γ-rings during carotenoid biosynthesis (*56*). In general, it is believed that the class of enzymes termed terpenoid cyclases catalyzes a number of complex cyclization reactions involving carbocation intermediates (*57*). The experiments presented in these studies suggest that a carbocation can be well-stabilized by the active site of an enzyme until complex transformations occur. Isomerization of *all-trans*-retinol could be another example of the reaction that occurs with the formation of a carbocation intermediate.

Possible Mechanism of all-trans-Retinol Isomerization via a Carbocation Intermediate. In light of these observations, we would like to propose a novel mechanism involved in the regeneration of opsin chromophore, 11-*cis*-retinal. *all-trans*-Retinol from ROS diffuses to the RPE cells, where it is esterified by the enzymatic activity of LRAT to form retinyl esters, the majority of which is *all-trans*-retinyl palmitate. Retinyl esters are then hydrolyzed by a hydrolase to the less stable free retinol. Both the hydrolase and isomerase reactions could be physically separated processes but occurring subsequently one after another in an enzymatic complex. By the action of isomerase, the hydroxy group of *all-trans*-retinol is protonated, and elimination of water from the unstable oxonium ion leads to the formation of an *all-trans*-retinyl carbocation. The carbocation exists as a mixture of resonance structures where the positive charge is delocalized within the polyene chain (Figure 9), producing a lower energetic barrier for the *trans*−*cis* isomerization. Hydration of carbocation isomers with subsequent expulsion of a proton leads to the formation of different isomers of retinol depending on the specificity of the retinoid-binding proteins present in the assays. Thus, in the presence of 11-*cis*-specific CRALBP, 11-*cis*-retinol is formed, and 11-*cis*- and 13-*cis*-retinol are formed in the presence of CRBP.

ACKNOWLEDGMENT

We thank Preston Van Hooser for excellent assistance, Dr. Martin Sadilek for assistance with MS analysis, and Dr. Donald Zack (Johns Hopkins University) for the RPE library.

REFERENCES

1. Palczewski, K., Polans, A., Baehr, W., and Ames, J. B. (2000) *BioEssays 22*, 337−350.
2. Polans, A., Baehr, W., and Palczewski, K. (1996) *Trends Neurosci. 19*, 547−554.
3. Lagndao, L., and Baylor, D. (1992) *Neuron 8*, 995−1002.
4. Koutalos, Y., and Yau, K. W. (1996) *Trends Neurosci. 19*, 73−81.
5. Pugh, E. N., Jr., Nikonov, S., and Lamb, T. D. (1999) *Curr. Opin. Neurobiol. 9*, 410−418.
6. Allikmets, R., Singh, N., Sun, H., Shroyer, N. E., Hutchinson, A., Chidambaram, A., Gerrard, B., Baird, L., Stauffer, D., Peiffer, A., Rattner, A., Smallwood, P., Li, Y. X., Anderson, K. L., Lewis, R. A., Nathans, J., Leppert, M., Dean, M., and Lupski, J. R. (1997) *Nat. Genet. 15*, 236−246.
7. Illing, M., Molday, L. L., and Molday, R. S. (1997) *J. Biol. Chem. 272*, 10303−10310.
8. Sun, H., Molday, R. S., and Nathans, J. (1999) *J. Biol. Chem. 274*, 8269−8281.
9. Weng, J., Mata, N. L., Azarian, S. M., Tzekov, R. T., Birch, D. G., and Travis, G. H. (1999) *Cell 98*, 13−23.
10. Zimmerman, W. H., Yost, M. T., and Daemen, F. J. M. (1974) *Nature 250*, 66−67.
11. Saari, J. C., Garwin, G. G., Van Hooser, J. P., and Palczewski, K. (1998) *Vision Res. 38*, 1325−1333.
12. Wald, G., and Hubbard, R. (1949) *J. Gen. Physiol. 32*, 367−389.
13. Futterman, S., Hendrickson, A., Bishop, P. E., Rollins, M. H., and Vacano, E. (1970) *J. Neurochem. 17*, 149−156.
14. De Pont, J. J., Daemen, F. J., and Bonting, S. L. (1970) *Arch. Biochem. Biophys. 140*, 275−285.
15. Lion, F., Rotmans, J. P., Daemen, F. J. M., and Bonting, S. L. (1975) *Biochim. Biophys. Acta 384*, 283−292.
16. Nicotra, C., and Livrea, M. A. (1982) *J. Biol. Chem. 257*, 11836−11841.
17. Palczewski, K., Jager, S., Buczylko, J., Crouch, R. K., Bredberg, D. L., Hofmann, K. P., Asson-Batres, M. A., and Saari, J. C. (1994) *Biochemistry 33*, 13741−13750.
18. Haeseleer, F., Huang, J., Lebioda, L., Saari, J. C., and Palczewski, K. (1998) *J. Biol. Chem. 273*, 21790−21799.
19. Rattner, A., Smallwood, P. M., and Nathans, J. (2000) *J. Biol. Chem. 275*, 11034−11043.
20. Bok, D. (1993) *J. Cell Sci. 17*, 189−195.
21. Palczewski, K., Van Hooser, J. P., Garwin, G. G., Chen, J., Liou, G. I., Saari, J. C. (1999) *Biochemistry 38*, 12012−12019.
22. MacDonald, P. N., and Ong, D. E. (1988) *Biochem. Biophys. Res. Commun. 156*, 157−163.
23. MacDonald, P. N., and Ong, D. E. (1988) *J. Biol. Chem. 263*, 12478−12482.
24. Saari, J. C., and Bredberg, D. L. (1989) *J. Biol. Chem. 264*, 8636−8640.
25. Saari, J. C., and Bredberg, D. L. (1990) *Methods Enzymol. 190*, 156−163.
26. Ruiz, A., Winston, A., Lim, Y.-H., Gilbert, B. A., Rando, R. R., and Bok, D. (1999) *J. Biol. Chem. 274*, 3834−3841.
27. Deigner, P. S., Law, W. C., Canada, F. J., and Rando, R. R. (1989) *Science 244*, 968−971.
28. Mata, J. R., Mata, N. L., and Tsin, A. T. C. (1998) *J. Lipid Res. 39*, 604−612.
29. Mata, N. L., Villazana, E. T. and Tsin, A. T. C. (1998) *Invest. Ophthalmol. Vis. Sci. 39*, 1312−1319.

30. Winston, A., and Rando, R. R. (1998) *Biochemistry 37*, 2044−2050.
31. Stecher, H., Gelb, M. H., Saari, J. C., and Palczewski, K. (1999) *J. Biol. Chem. 274*, 8577−8585.
32. Stecher, H., Prezhdo, O., Das, J., Crouch, R. K., and Palczewski, K. (1999) *Biochemistry 38*, 13542−13550.
33. Stecher, H., and Palczewski, K. (2000) *Methods Enzymol. 316*, 330−344.
34. Simon, A., Hellman, U., Wernstedt, C., and Eriksson, U. (1995) *J. Biol. Chem. 270*, 1107−1112.
35. Driessen, C. A., Winkens, H. J., Kuhlmann, E. D., Janssen, A. P., van Vugt, A. H. M., Deutman, A. F., and Janssen, J. J. (1998) *FEBS Lett. 428*, 135−140.
36. Driessen, C. A., Winkens, H. J., Hoffmann, K., Kuhlmann, E. D., Janssen, A. P., Van Vugt, A. H., Van Hooser, J. P., Wieringa, B. E., Deutman, A. F., Palczewski, K., Ruether, K., and Janssen, J. J.. (2000) *Mol. Cell. Biol. 20*, 897−908.
37. Yamamoto, H., Simon, A., Eriksson, U., Harris, E., Berson, E. L., and Dryja, T. P. (1999) *Nat. Genet. 22*, 188−191.
38. Cideciyan, A.V., Haeseleer, F., Fariss, R. N., Aleman, T. S., Jang, G. F., Verlinde, C. L., Marmor, M. F., Jacobson, S. G., and Palczewski, K. (2000) *Vis. Neurosci. 17*, 513−533.
39. Gonzalez-Fernandez, F., Kurz, D., Bao, Y., Newman, S., Conway, B. P., Young, J. E., Han, D. P., and Khani, S. C. (1999) *Mol. Vision 5*, 41.
40. Crouch, R. K., Chader, G. J., Wiggert, B., and Pepperberg, D. R. (1996) *Photochem. Photobiol. 64*, 613−621.
41. Gu, S. M., Thompson, D. A., Srikumari, C. R., Lorenz, B., Finckh, U., Nicoletti, A., Murthy, K. R., Rathmann, M., Kumaramanickavel, G., Denton, M. J., and Gal, A. (1997) *Nat. Genet. 17*, 194−197.
42. Morimura, H., Fishman, G. A., Grover, S. A., Fulton, A. B., Berson, E. L., Dryja, T. P. (1998) *Proc. Natl. Acad. Sci. U.S.A. 95*, 3088−3093.
43. Perrault, I., Rozet, J. M., Gerber, S., Ghazi, I., Leowski, C., Ducroq, D., Souied, E., Dufier, J. L., Munnich, A., and Kaplan, J. (1999) *Mol. Genet. Metab. 68*, 200−208.
44. Saari, J. C., Nawrot, M., Hurley, J. B., Garwin, G. G., Huang, J., Crabb, J. W. (2000) *Invest. Ophthalmol. Vis. Sci. 41*, 533.
45. Bradford, M. M. (1976) *Anal. Biochem. 72*, 248−254.
46. Garwin, G. G., and Saari, J. C. (2000) *Methods Enzymol. 316*, 313−324.
47. Francesch, A., Alvarez, R., Lòpez, S., de Lera, A. R. (1997) *J. Org. Chem. 62*, 310−319.
48. Crabb, J. W., Chen, Y., Goldflam, S., West, K., and Kapron, J. (1998) in *Methods in Molecular Biology: Retinoid Protocols* (Redfern, C. P. F., Ed.), Vol 89, pp 91−104, Humana Press, Totowa, NJ.
49. Alvarez, R., Iglesias, B., López, S., and de Lera, A. R. (1998) *Tetrahedron Lett. 39*, 5659−5662.
50. Bhat, P. V., Roller, P. P., De Luca, L. M. (1981) *J. Lipid Res. 22*, 1069−1078.
51. March, J. (1985) in *Advanced Organic Chemistry*, 3rd ed., John Wiley & Sons Inc, New York.
52. Pienta, N. J., Kessler, R. J. (1992) *J. Am. Chem. Soc. 114*, 2419−2428.
53. Rando, R. R. (1996) *Chem. Biol. 3*, 255−262.
54. Saari, J. C., Bredberg, D. L., and Garwin, G. G. (1982) *J. Biol. Chem. 257*, 13329−13333.
55. Lesburg, C. A., Zhai, G., Cane, D. E., Christianson, D. W. (1997) *Science 277*, 1820−1824.
56. Bouvier, F., d'Harlingue, A., Camara, B. (1997) *Arch. Biochem. Biophys. 346*, 53−64.
57. Lesburg, C. A., Caruthers, J. M., Paschall, C. M., Christianson, D. W. (1998) *Curr. Opin. Struct. Biol. 8*, 695−703.

BI001061C